Impact Factor:					
	ISRA (India) = 4.971	SIS (USA) = 0.912	ICV (Poland) = 6.630
	ISI (Dubai, UAE) = 0.829	РИНЦ (Russia) = 0.126	PIF (India) = 1.940
	GIF (Australia) = 0.564	ESJI (KZ) = 8.997	IBI (India) = 4.260
	JIF = 1.500	SJIF (Morocco) = 5.667	OAJI (USA) = 0.350

SOI: 1.1/TAS DOI: 10.15863/TAS

International Scientific Journal

Theoretical & Applied Science

p-ISSN: 2308-4944 (print) **e-ISSN:** 2409-0085 (online)

Year: 2020 **Issue:** 10 **Volume:** 90

Published: 28.10.2020 **http://T-Science.org**

QR – Issue QR – Article

Denis Chemezov
Vladimir Industrial College
M.Sc.Eng., Corresponding Member of International Academy of Theoretical and Applied Sciences, Lecturer, Russian Federation
https://orcid.org/0000-0002-2747-552X
vic-science@yandex.ru

Lyubov Suvorova
Vladimir Industrial College
Student, Russian Federation

Aleksey Kuznetsov
Vladimir Industrial College
Student, Russian Federation

Elena Bogomolova
Vladimir Industrial College
Materials Developer, Lecturer, Russian Federation

Aleksey Kuzmichev
Vladimir Industrial College
Head of Workshops, Russian Federation

Irina Pavlukhina
Vladimir Industrial College
Lecturer, Russian Federation

Andrey Komissarov
Vladimir Industrial College
Master of Industrial Training, Russian Federation

COMPARATIVE ANALYSIS OF CHARACTERISTICS OF WATER AND INDUSTRIAL OIL FLOWS IN THE PIPELINE WITH THE DIFFUSER

Abstract: *The computer calculation of water and industrial oil flow in the pipeline with the diffuser was implemented in the article. Comparison of changing the cell Reynolds number, pressure, and velocity of fluids flow in the conditions of laminar and turbulent regimes was made. It is found that characteristics of fluids during laminar flow and turbulent flows according to the Algebraic yPlus and L-VEL models are almost identical. Maximum intensity of the vortex flows formation is observed at the outlet of the expanding part of the pipeline during laminar water flow and according to the Algebraic yPlus, L-VEL and Spalart-Allmaras turbulence models. Flow of industrial oil in the pipeline with the diffuser practically does not lead to the vortex flows formation.*

Key words: *water, industrial oil, the pipeline, laminar flow, the turbulence model, the diffuser, velocity.*

Language: *English*

Citation: Chemezov, D., et al. (2020). Comparative analysis of characteristics of water and industrial oil flows in the pipeline with the diffuser. *ISJ Theoretical & Applied Science, 10 (90),* 368-380.

Soi: http://s-o-i.org/1.1/TAS-10-90-64 ***Doi***: crossref https://dx.doi.org/10.15863/TAS.2020.10.90.64

Introduction

The transition process from laminar regime of fluid flow to turbulent regime is visually displayed during the calculation in the special computer programs. Laminar regime is characterized by moving the fluid layers in one direction at variable velocity at the distance from the axial line to the pipeline wall. Turbulent (transient) regime occurs when fluid flow through the hydraulic resistance [1-2]. In this case, changing the flow direction of the fluid layers, their mixing and the vortices formation of various intensities occur [3-4]. The calculation of turbulent flow of fluids is carried out by the turbulence models [5-7]. The turbulence models based on the Reynolds equation are characterized by the different descriptions of fluid flow in the wall region (the pipeline) and the number of the additional variables.

The Algebraic yPlus and L-VEL turbulence models, which have the highest stability and the lower accuracy, are used for the calculation of the coefficient of turbulent viscosity depending on flow velocity of fluid and the distance from the wall. The *k-ε* turbulence model, which is characterized by the fast convergence and the low accuracy in modeling the some hydraulic problems, includes the equation of turbulence kinetic energy and the equation of kinetic energy dissipation rate. The model is well suited for solving the problems of external flow around bodies. In the *k-ω* turbulence model, which is characterized by the low convergence and sensitivity to the initial approximation, the second parameter is calculated from the equation of specific rate of kinetic energy dissipation [8]. The accurate results for this model can be obtained by modeling fluid flow through curved channels. The Spalart-Allmaras turbulence model, which is characterized by stability and the good convergence, is used for the calculation of the kinematic coefficient of vortex viscosity of fluid flowing in the entire domain, including the wall layers [9-10]. The SST turbulence model is the improved combination of the *k-ε* and *k-ω* turbulence models.

The diffuser (the hydraulic resistance), which is the expanding section of the pipeline, is used to slow down flow of fluid. Using the turbulence models listed above and the laminar flow equation for the calculation, you can get the visual presentation of changing the parameters of fluid flow before the hydraulic resistance, along the diffuser length, and at the certain distance after the hydraulic resistance.

Materials and methods

The computer experiment to determine the characteristics of laminar and turbulent flows of fluids in the pipeline with the diffuser is implemented in the Comsol Multiphysics program. The models of water and industrial oil at atmospheric pressure and the temperature of 20 °C were used as working fluids. The discretization of fluids was given as P1+P1. The properties of water and industrial oil for modeling are presented in the tables 1-2.

Table 1. The properties of water at atmospheric pressure and the temperature of 20 °C.

Parameter	Unit of measurement	Value
Density	kg/m^3	998.2
Specific enthalpy	kJ/kg	83.91
Specific heat	kJ/(kg·°C)	4183
Thermal conductivity	W/(m·°C)	0.599
Diffusivity	m^2/s	14.3
Dynamic viscosity	Pa·s	1004
Kinematic viscosity	m^2/s	1.006
Coefficient of thermal volumetric expansion	$°C^{-1}$	1.82
Surface tension coefficient	N/m	726.9
Prandtl number		7.02

Table 2. The properties of industrial oil at atmospheric pressure and the temperature of 20 °C.

Parameter	Unit of measurement	Value
Density	kg/m^3	865
Kinematic viscosity	m^2/s	0.00003132
Flash point	°C	206
Pour point	°C	-15

The pipeline model with the diffuser had the following dimensions: the inner diameter at the inlet was 80 mm, the length of the cylindrical section before expansion was 60 mm, the inner diameter at the outlet was 160 mm, the length of the cylindrical section after expansion was 200 mm, the angle of the

expanding part was 18 deg., the length of the expanding part was 120 mm. The *X*-axis contours on the pipeline model were the wall, and the *Y*-axis contours were the inlet and the outlet. Initial velocity of fluids flow at the inlet was adopted 1 m/s. Flow time of fluids in the pipeline was adopted 1 s. Flow of fluids occurred in the conditions of laminar and turbulent regimes. Turbulent flows of fluids were calculated according to the models:

1. Algebraic yPlus – two constant parameters are set: k_a (0.402) and B_a (6.59);

2. L-VEL – two constant parameters are set: k_l (0.417) and E_l (8.6);

3. k-ε – seven constant parameters are set: $C_{\varepsilon 1}$ (1.44), $C_{\varepsilon 2}$ (1.92), C_μ (0.09), σ_k (1), σ_ε (1.3), k_v (0.41) and B (5.2);

4. k-ω – seven constant parameters are set: α (13/25), σ_k^* (1/2), σ_ω (1/2), β_0 (9/125), β_0^* (9/100), k_v (0.41) and B (5.2);

5. Spalart-Allmaras – eight constant parameters are set: C_{b1} (0.1355), C_{b2} (0.622), C_{v1} (7.1), $\sigma_{\tilde{v}}$ (2/3), C_{w2} (0.3), C_{w3} (2), k_v (0.41) and C_{Rot} (2).

The boundary conditions for laminar and turbulent flows of water and industrial oil in the pipeline with the diffuser are presented in the Fig. 1 and the tables 3-8.

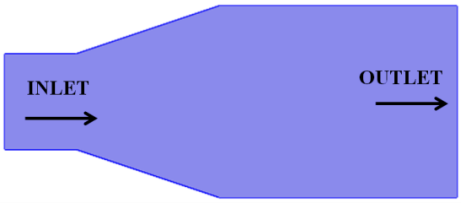

Figure 1 – The boundary conditions for the modeling the process of fluids flow in the pipeline with the diffuser.

Table 3. The boundary conditions for laminar flow of fluids.

Parameters	**Equations**
Main conditions	$\rho\frac{\partial u}{\partial t}+\rho(u\cdot\nabla)u=\nabla\cdot\left[-pI+\mu\left(\nabla u+(\nabla u)^T\right)\right]+F$ $\rho\nabla\cdot(u)=0$
Wall	$u=0$
Inlet	$u=-U_0 n$
Outlet	$\left[-pI+\mu\left(\nabla u+(\nabla u)^T\right)\right]n=-\hat{p}_0 n$ $\hat{p}_0\le p_0$

Table 4. The boundary conditions for turbulent flow of fluids according to the Algebraic yPlus model.

Parameters	**Equations**
Main conditions	$\rho\frac{\partial u}{\partial t}+\rho(u\cdot\nabla)u=\nabla\cdot\left[-pI+(\mu+\mu_T)\left(\nabla u+(\nabla u)^T\right)\right]+F$ $\rho\nabla\cdot(u)=0$
Wall	$u=0$
Inlet	$u=-U_0 n$
Outlet	$\left[-pI+(\mu+\mu_T)\left(\nabla u+(\nabla u)^T\right)\right]n=-\hat{p}_0 n$ $\hat{p}_0\le p_0$

Table 5. The boundary conditions for turbulent flow of fluids according to the L-VEL model.

Parameters	**Equations**
Main conditions	$\rho\frac{\partial u}{\partial t}+\rho(u\cdot\nabla)u=\nabla\cdot\left[-pI+(\mu+\mu_T)\left(\nabla u+(\nabla u)^T\right)\right]+F$ $\rho\nabla\cdot(u)=0$
Wall	$u=0$

Inlet	$u = -U_0 n$
Outlet	$\left[-pI + (\mu + \mu_T)(\nabla u + (\nabla u)^T)\right] n = -\hat{p}_0 n$ $\hat{p}_0 \le p_0$

Table 6. The boundary conditions for turbulent flow of fluids according to the *k-ε* model.

Parameters	**Equations**
Main conditions	$\rho \frac{\partial u}{\partial t} + \rho(u \cdot \nabla)u = \nabla \cdot \left[-pI + (\mu + \mu_T)(\nabla u + (\nabla u)^T)\right] + F$ $\rho \nabla \cdot (u) = 0$ $\rho \frac{\partial k}{\partial t} + \rho(u \cdot \nabla)k = \nabla \cdot \left[\left(\mu + \frac{\mu_T}{\sigma_k}\right)\nabla k\right] + P_k - \rho\varepsilon$ $\rho \frac{\partial \varepsilon}{\partial t} + \rho(u \cdot \nabla)\varepsilon = \nabla \cdot \left[\left(\mu + \frac{\mu_T}{\sigma_\varepsilon}\right)\nabla \varepsilon\right] + C_{\varepsilon 1}\frac{\varepsilon}{k}P_k - C_{\varepsilon 2}\rho\frac{\varepsilon^2}{k}$ $\varepsilon = ep$ $\mu_T = \rho C_\mu \frac{k^2}{\varepsilon}$ $P_k = \mu_T\left[\nabla u : (\nabla u + (\nabla u)^T)\right]$
Wall	$u \cdot n = 0$ $\left[(\mu + \mu_T)(\nabla u + (\nabla u)^T)\right] n = -\rho \frac{u_\tau}{\delta_w^+} u_{\tan g}$ $u_{\tan g} = u - (u \cdot n)n$ $\nabla k \cdot n = 0$ $\varepsilon = \rho \frac{C_\mu k^2}{k_v \delta_w^+ \mu}$
Inlet	$u = -U_0 n$ $U_{ref} = U_0$ $k = \frac{3}{2}(U_{ref} I_T)^2$ $\varepsilon = C_\mu^{3/4}\frac{k^{3/2}}{L_T}$
Outlet	$\left[-pI + (\mu + \mu_T)(\nabla u + (\nabla u)^T)\right] n = -\hat{p}_0 n$ $\hat{p}_0 \le p_0$ $\nabla k \cdot n = 0$ $\nabla \varepsilon \cdot n = 0$

Table 7. The boundary conditions for turbulent flow of fluids according to the *k-ω* model.

Parameters	**Equations**
Main conditions	$\rho \frac{\partial u}{\partial t} + \rho(u \cdot \nabla)u = \nabla \cdot \left[-pI + (\mu + \mu_T)(\nabla u + (\nabla u)^T)\right] + F$ $\rho \nabla \cdot (u) = 0$ $\rho \frac{\partial k}{\partial t} + \rho(u \cdot \nabla)k = \nabla \cdot \left[(\mu + \mu_T \sigma_k^*)\nabla k\right] + P_k - \beta_0^* \rho \omega k$ $\rho \frac{\partial \omega}{\partial t} + \rho(u \cdot \nabla)\omega = \nabla \cdot \left[(\mu + \mu_T \sigma_\omega)\nabla \omega\right] + \alpha \frac{\omega}{k} P_k - \rho \beta_0 \omega^2$ $\omega = om$

	$\mu_T = \rho\frac{k}{\omega}$ $P_k = \mu_T\left[\nabla u : \left(\nabla u + (\nabla u)^T\right)\right]$
Wall	$u \cdot n = 0$ $\left[\left(\mu + \mu_T\right)\left(\nabla u + (\nabla u)^T\right)\right]n = -\rho\frac{u_\tau}{\delta_w^+}u_{\tan g}$ $u_{\tan g} = u - (u \cdot n)n$ $\nabla k \cdot n = 0$ $\omega = \rho\frac{k}{k_v\delta_w^+\mu}$
Inlet	$u = -U_0 n$ $U_{ref} = U_0$ $k = \frac{3}{2}\left(U_{ref}I_T\right)^2$ $\omega = \frac{k^{1/2}}{\left(\beta_0^*\right)^{1/4}L_T}$
Outlet	$\left[-pI + \left(\mu + \mu_T\right)\left(\nabla u + (\nabla u)^T\right)\right]n = -\hat{p}_0 n$ $\hat{p}_0 \le p_0$ $\nabla k \cdot n = 0$ $\nabla\omega \cdot n = 0$

Table 8. The boundary conditions for turbulent flow of fluids according to the Spalart-Allmaras model.

Parameters	**Equations**
Main conditions	$\rho\frac{\partial u}{\partial t} + \rho(u \cdot \nabla)u = \nabla \cdot \left[-pI + \left(\mu + \mu_T\right)\left(\nabla u + (\nabla u)^T\right)\right] + F$ $\rho\nabla \cdot (u) = 0$ $\frac{\partial \nu^t}{\partial t} + (u \cdot \nabla)\nu^t = C_{b1}S^t\nu^t - C_{w1}f_w\left(\frac{\nu^t}{l_w}\right)^2 + \frac{1}{\sigma_{\tilde{\nu}}}\nabla \cdot \left(\left(\nu + \nu^t\right)\nabla\nu^t\right) + \frac{C_{b2}}{\sigma_{\tilde{\nu}}}\nabla\nu^t \cdot \nabla\nu^t$ $\nu^t = nutilde$ $\nabla G \cdot \nabla G + \sigma_\omega G(\nabla \cdot \nabla G) = (1 + 2\sigma_\omega)G^4$ $l_\omega = \frac{1}{G} - \frac{l_{ref}}{2}$ $\mu_T = \rho\nu^t f_{v1}$ $C_{w1} = \frac{C_{b1}}{k_v^2} + \frac{1 + C_{b2}}{\sigma_{\tilde{\nu}}}$ $f_{v1} = \frac{\chi^3}{\chi^3 + C_{v1}^3}$ $f_{v2} = 1 - \frac{\chi}{1 + \chi f_{v1}}$ $\chi = \frac{\nu^t}{\nu}$ $f_w = g\left(\frac{1 + C_{w3}^6}{g^6 + C_{w3}^6}\right)$ $g = r + C_{w2}\left(r^6 - r\right)$

	$r = \min\left(\frac{\nu^t}{S^t k_v^2 l_w^2}, 10\right)$ $S^t = \max\left(\Omega + C_{Rot}\min(0, S-\Omega) + \frac{\nu^t}{k_v^2 l_w^2} f_{v2}, 0.3\Omega\right)$ $\Omega = \sqrt{2\Omega : \Omega}$ $S = \sqrt{2S : S}$ $\Omega = \frac{1}{2}\left(\nabla u - (\nabla u)^T\right)$ $S = \frac{1}{2}\left(\nabla u + (\nabla u)^T\right)$
Wall	$u = 0$ $\nu^t = 0$ $G = \frac{2}{l_{ref}}$
Inlet	$u = -U_0 n$ $U_{ref} = U_0$ $\nu^t = \nu_0$ $\nabla G \cdot n = 0$
Outlet	$\left[-pI + (\mu + \mu_T)\left(\nabla u + (\nabla u)^T\right)\right]n = -\hat{p}_0 n$ $\hat{p}_0 \le p_0$ $\nabla \nu^t \cdot n = 0$ $\nabla G \cdot n = 0$

where ρ – density; u – the velocity field; t – time; p – pressure; I – the unit tensor; μ – dynamic viscosity; ∇u – the gradient of the velocity field; T – the temperature; F – the volume force; U_0 – normal inflow speed; n – the boundary normal pointing out of the domain; $\hat{p}_0$ – pressure for suppress backflow; p_0 – prescribed pressure at the boundary; μ_T – turbulent viscosity; k – turbulent kinetic energy; σ_k – the model constant, 1.0; ∇k – the gradient of turbulent kinetic energy; P_k – the production term; ε – turbulent dissipation rate; σ_ε – the model constant, 1.3; $\nabla\varepsilon$ – the gradient of turbulent dissipation rate; $C_{\varepsilon 1}$ – the model constant, 1.44; $C_{\varepsilon 2}$ – the model constant, 1.92; C_μ – the model constant, 0.09; $:$ – contraction; u_τ – friction velocity; δ_w^+ – the wall lift-off in viscous units; u_{tang} – tangential velocity; k_v – the von Kárman constant, 0.41; U_{ref} – the reference velocity scale; I_T – turbulent intensity; L_T – the turbulence length scale; σ_k^* – the closure coefficient, 0.5; β_0^* – the closure coefficient, 9/100; ω – specific dissipation rate; σ_ω – the closure coefficient, 0.5; α – the closure coefficient, 13/25; β_0 – the closure coefficient, 9/125; $\nabla\omega$ – the gradient of specific dissipation rate; ν^t – the working variable of the turbulence model; C_{b1} – the model constant, 0.1355; S^t – magnitude of vorticity; C_{w1} – the model constant, $C_{b1}/k^2 + (1+C_{b2})/\sigma$; f_w – the non-dimensional function, which equal 1 in the log layer; l_w – the distance to the closest wall; $\sigma_{\tilde{\nu}}$ – the model constant, 2/3; $\nabla\nu^t$ – the gradient of the working variable of the turbulence model; C_{b2} – the model constant, 0.622; G – the reciprocal wall distance; l_{ref} – the reference length scale; f_{v1} – the function is borrowed from Mellor and Herring; χ – the intermediate variable; C_{v1} – the model constant, 7.1; f_{v2} – the function is constructed, just like f_{v1}, so that S^t maintains its log-layer behavior all way to the wall; g – the intermediate variable; C_{w3} – the model constant, 2; r – the intermediate variable; C_{w2} – the model constant, 0.3; Ω – the vorticity tensor; C_{Rot} – the model constant, 2; S – measure of the deformation tensor; v_0 – undamped turbulent kinematic viscosity.

Results and discussion

The contours of the cell Reynolds number, velocity, and pressure of water and industrial oil flow in the pipeline with the diffuser are presented in the Figs. 2-7. The maximum value for each parameter on the contours is red, and the minimum value is blue.

Flow regime of water and industrial oil in the pipeline with the diffuser with initial velocity of 1 m/s is laminar, since the calculated Reynolds number is less than 2300.

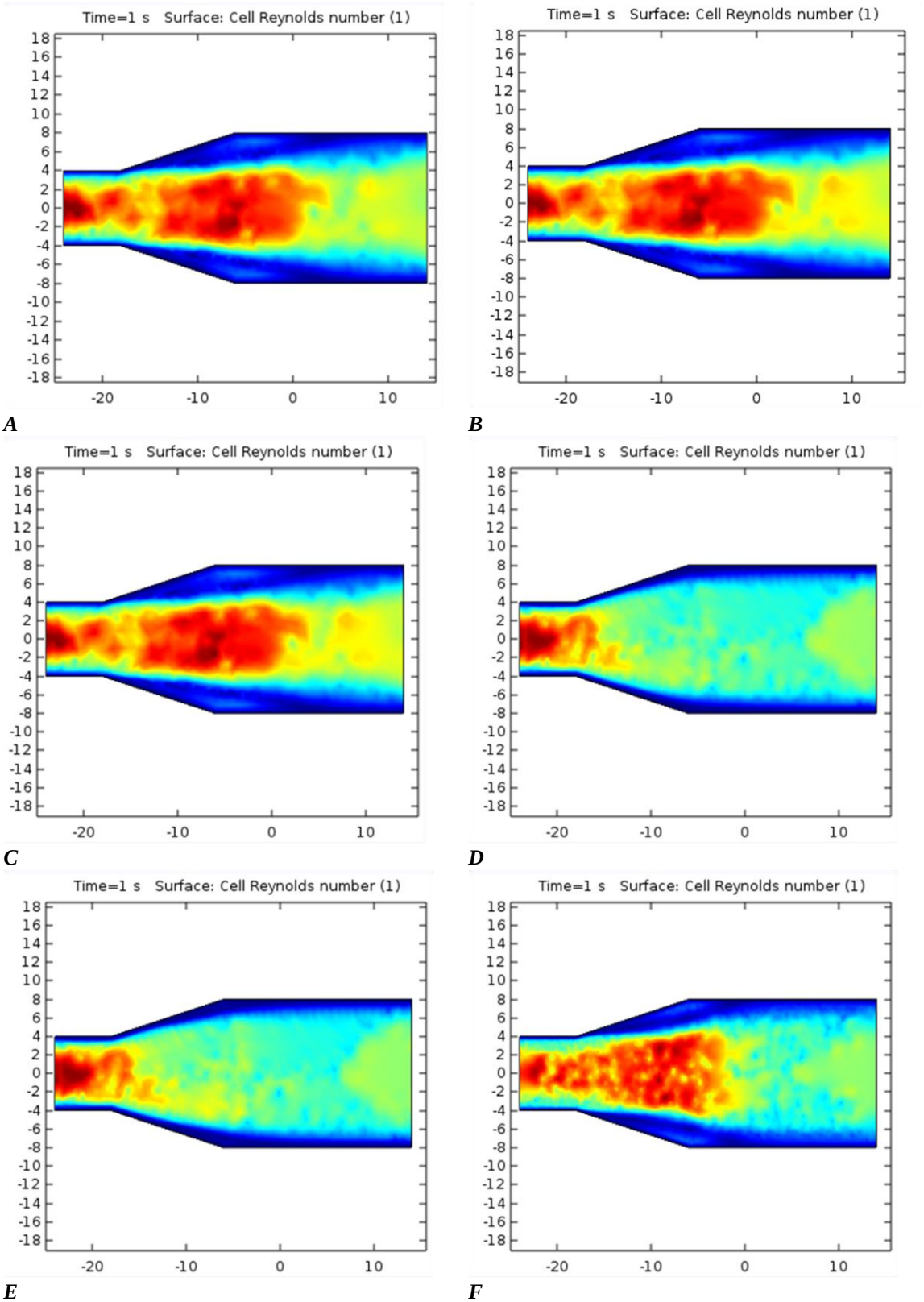

Figure 2 – The contours of the cell Reynolds number of water flow: *A* – laminar flow; *B* – turbulent flow according to the Algebraic yPlus model; *C* – turbulent flow according to the L-VEL model; *D* – turbulent flow according to the *k-ε* model; *E* – turbulent flow according to the *k-ω* model; *F* – turbulent flow according to the Spalart-Allmaras model.

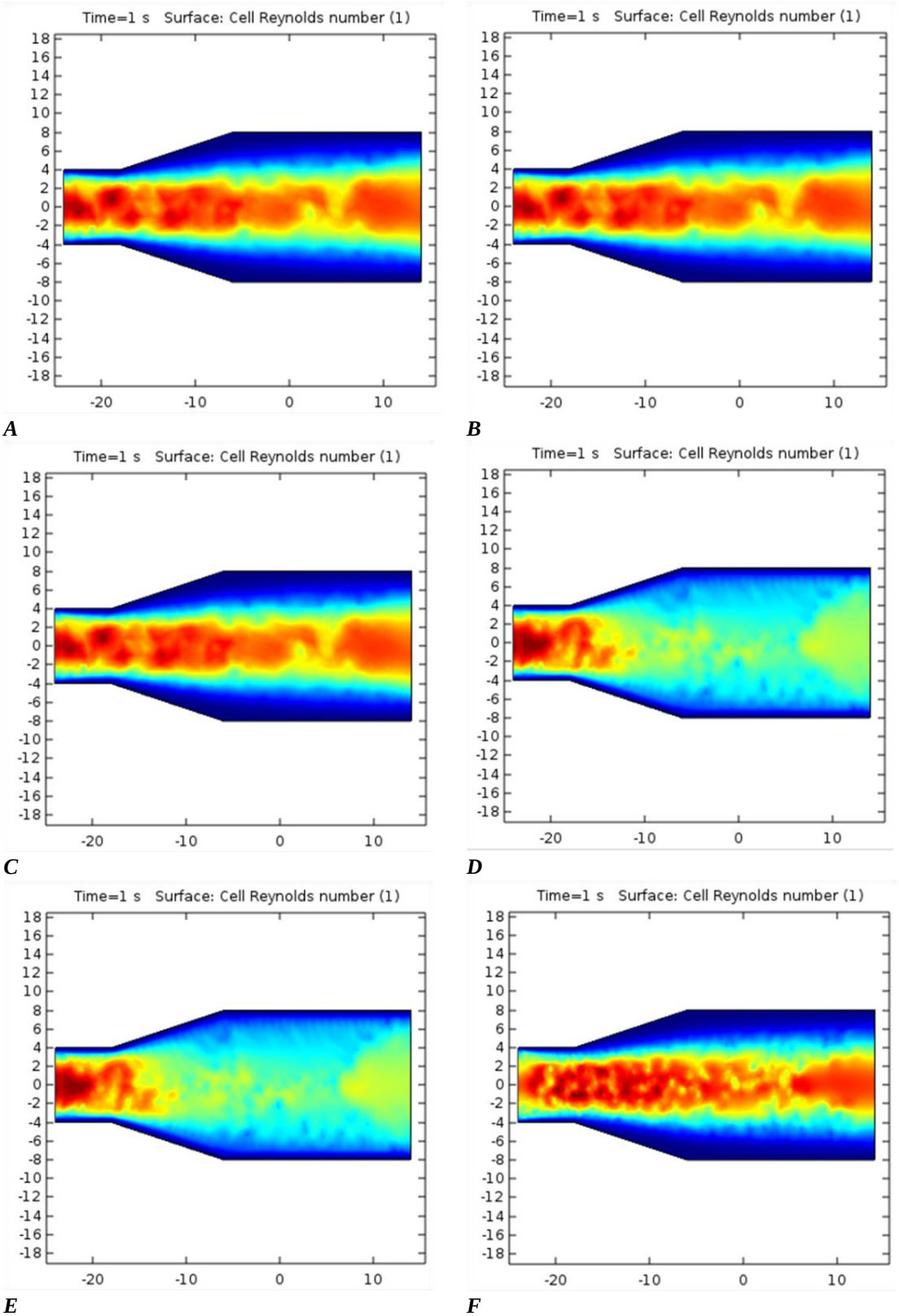

Figure 3 – The contours of the cell Reynolds number of industrial oil flow: *A* – laminar flow; *B* – turbulent flow according to the Algebraic yPlus model; *C* – turbulent flow according to the L-VEL model; *D* – turbulent flow according to the *k-ε* model; *E* – turbulent flow according to the *k-ω* model; *F* – turbulent flow according to the Spalart-Allmaras model.

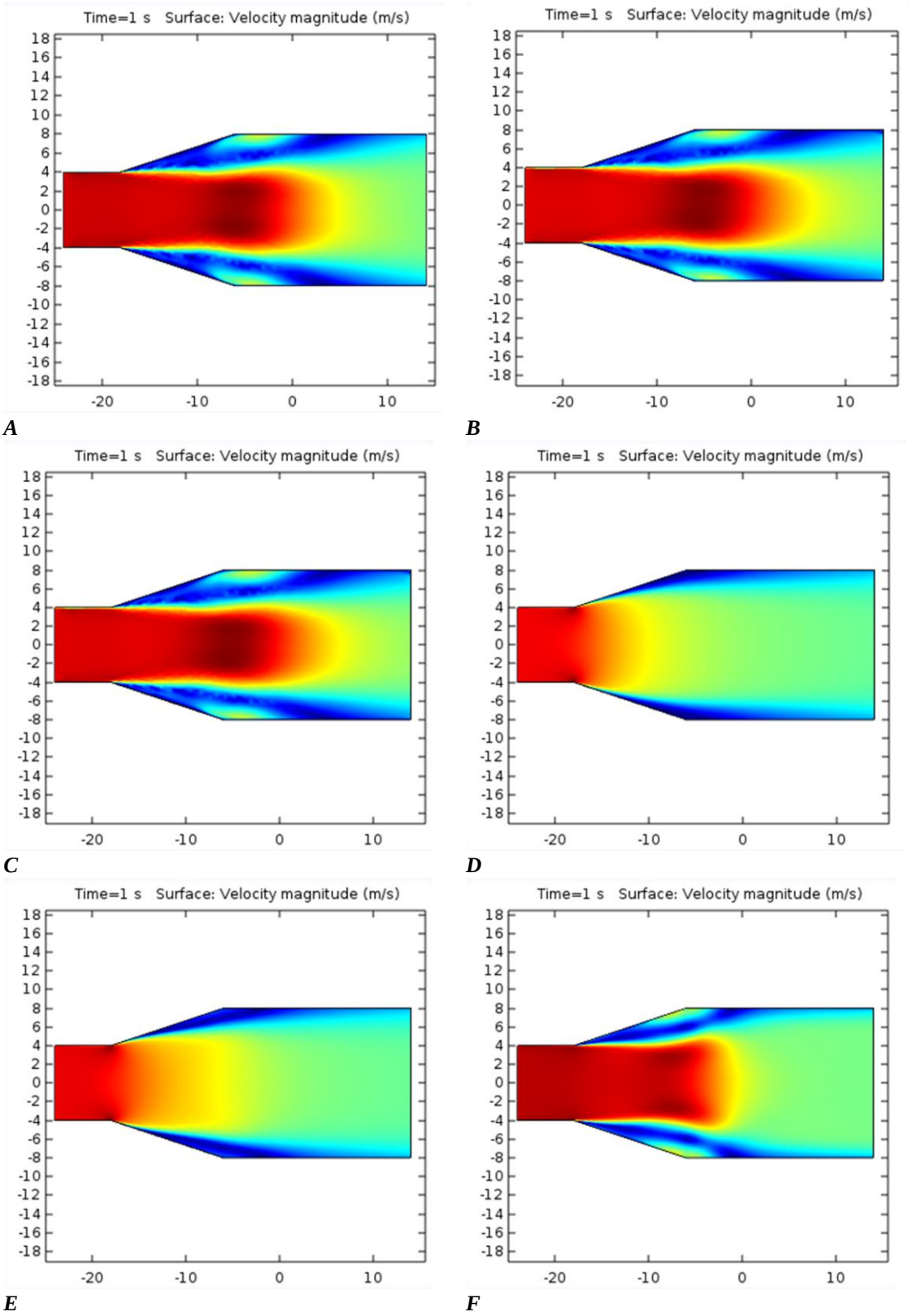

Figure 4 – The contours of flow velocity of water: *A* – laminar flow; *B* – turbulent flow according to the Algebraic yPlus model; *C* – turbulent flow according to the L-VEL model; *D* – turbulent flow according to the *k-ε* model; *E* – turbulent flow according to the *k-ω* model; *F* – turbulent flow according to the Spalart-Allmaras model.

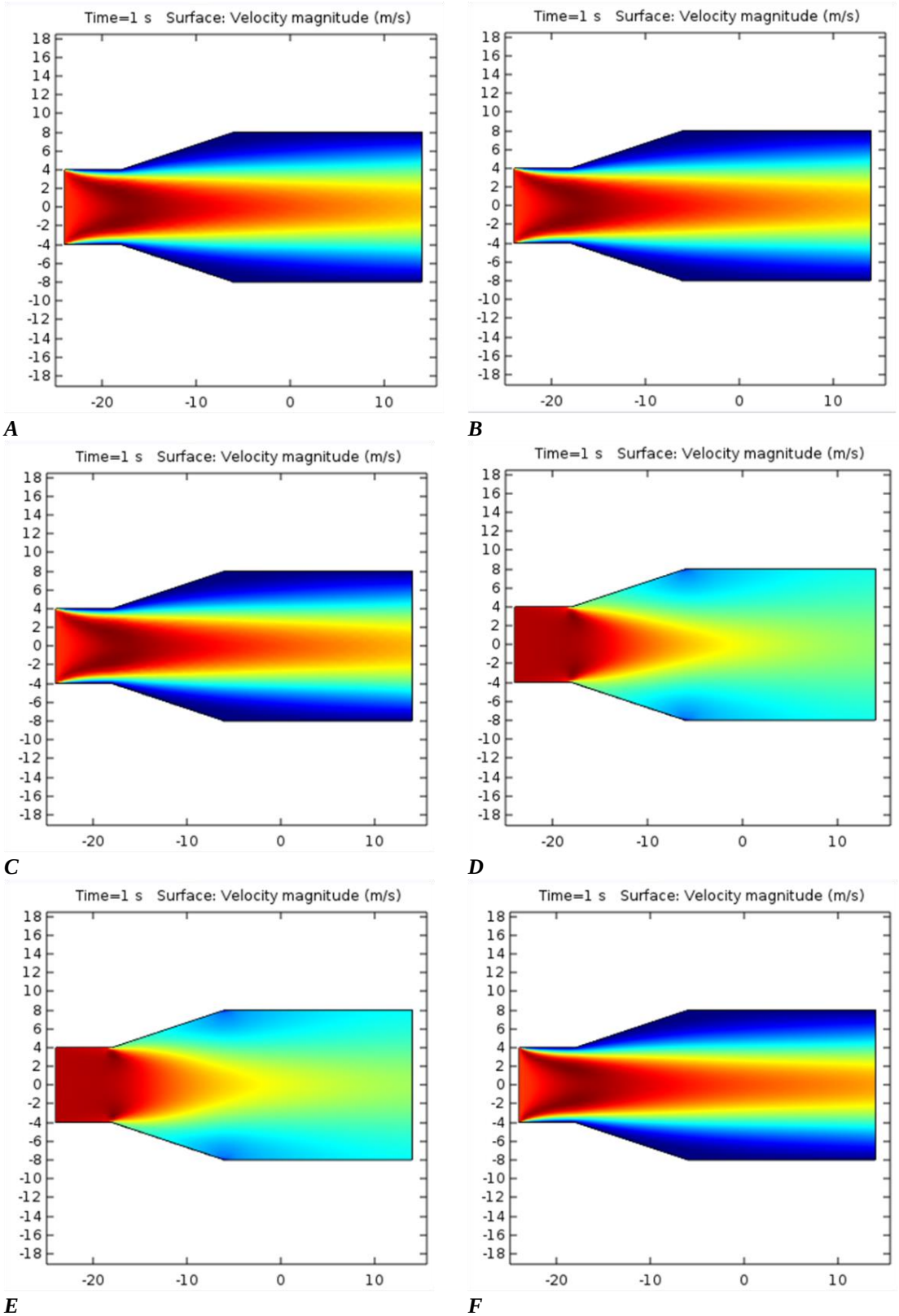

Figure 5 – The contours of flow velocity of industrial oil: *A* – laminar flow; *B* – turbulent flow according to the Algebraic yPlus model; *C* – turbulent flow according to the L-VEL model; *D* – turbulent flow according to the *k-ε* model; *E* – turbulent flow according to the *k-ω* model; *F* – turbulent flow according to the Spalart-Allmaras model.

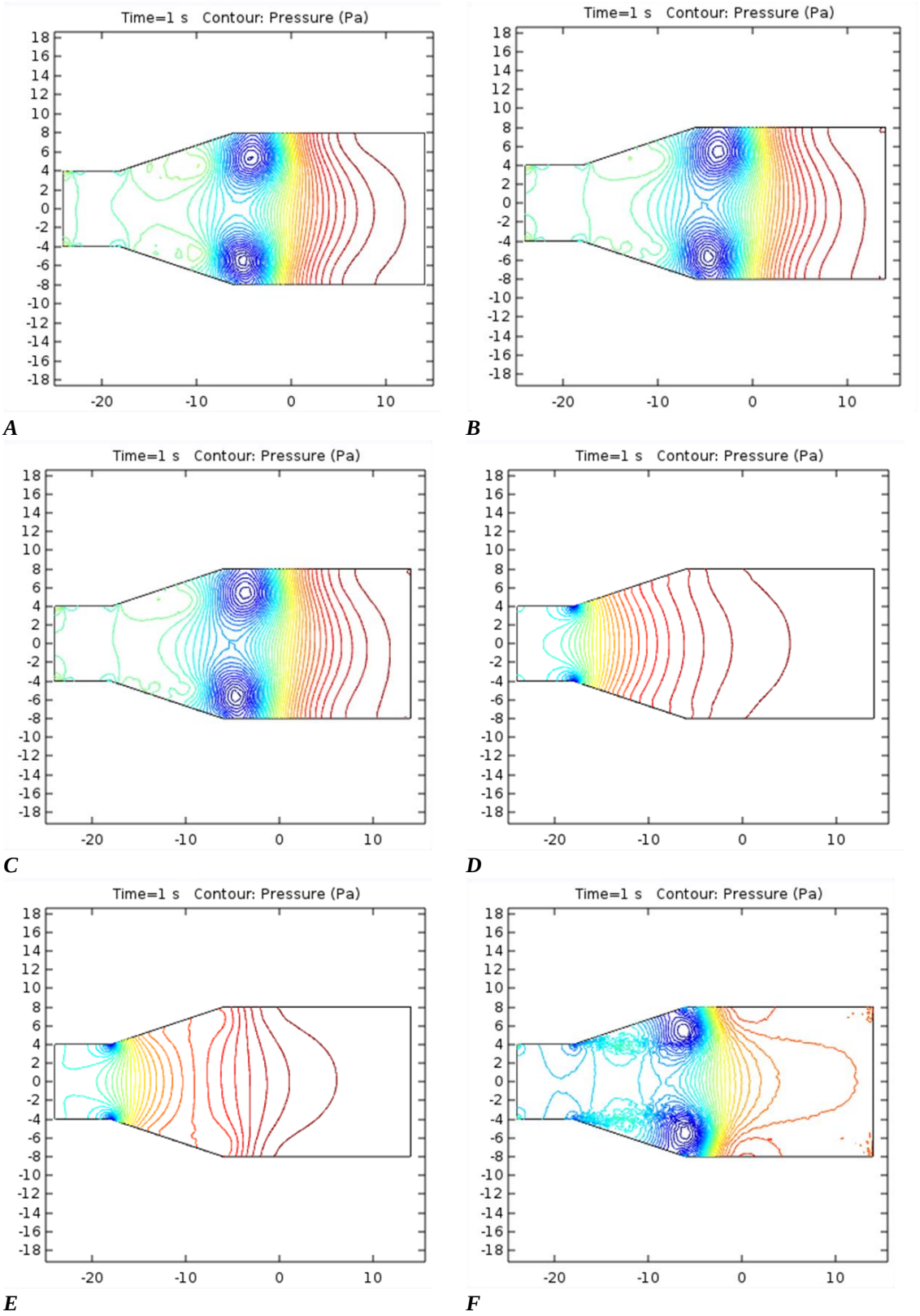

Figure 6 – The pressure contours of water flow: *A* – laminar flow; *B* – turbulent flow according to the Algebraic yPlus model; *C* – turbulent flow according to the L-VEL model; *D* – turbulent flow according to the *k-ε* model; *E* – turbulent flow according to the *k-ω* model; *F* – turbulent flow according to the Spalart-Allmaras model.

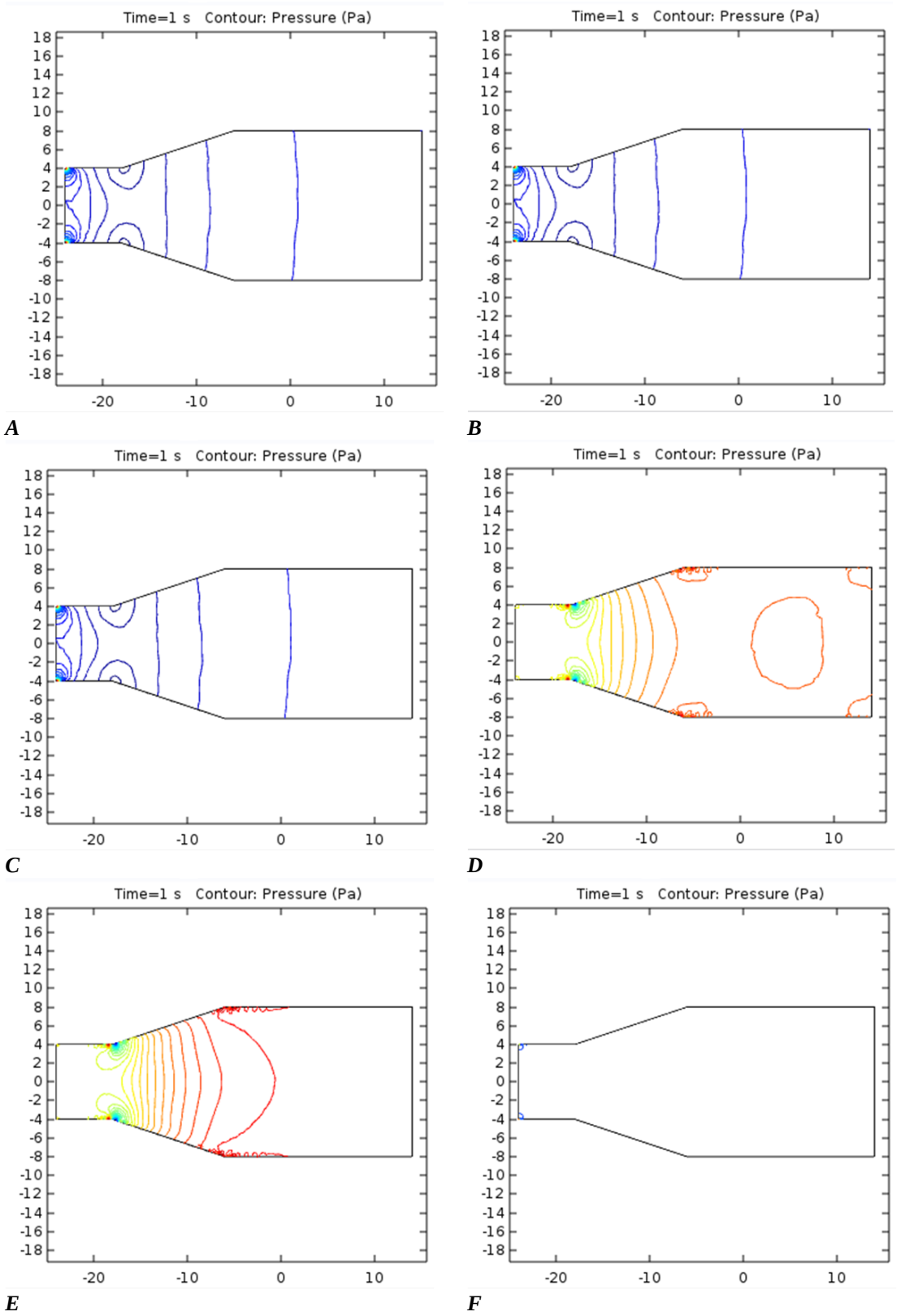

Figure 7 – The pressure contours of industrial oil flow: *A* – laminar flow; *B* – turbulent flow according to the Algebraic yPlus model; *C* – turbulent flow according to the L-VEL model; *D* – turbulent flow according to the *k-ε* model; *E* – turbulent flow according to the *k-ω* model; *F* – turbulent flow according to the Spalart-Allmaras model.

Let us consider flow of water in the pipeline. Flow velocity of water at the outlet of the diffuser increases by 8% relative to initial velocity. The maximum value of the Reynolds number in these conditions is 2105. The calculation according to the Algebraic yPlus and L-VEL turbulence models results in increasing flow velocity of fluid by 10% relative to initial velocity. The Reynolds number does not change. Flow velocities calculated according to the k-ε and k-ω turbulence models increase by 12% and 11%, respectively. However, the Reynolds number decreases by 1.6 times. The minimum values of flow velocity of water and the Reynolds number were determined at the calculation according to the Spalart-Allmaras turbulence model.

Let us consider flow of industrial oil in the pipeline. Flow of industrial oil is characterized by constant maximum velocity at the inlet to the diffuser in the conditions of the computer calculation according to the Algebraic yPlus, L-VEL, Spalart-Allmaras turbulence models and the laminar flow equation. It can be noted that maximum flow velocity of industrial oil increases by 10% compared to flow velocity of water. However, according to the *k-ε* and *k-ω* turbulence models was observed decreasing maximum flow velocity of industrial oil to initial velocity. The calculated values of the Reynolds number of industrial oil flow (from 1.30564 to 2.52396) indicate that it is impossible to the formation of vortex flows when fluid moves through the diffuser.

The formation of vortex flows occurs at the outlet of the diffuser (the pressure contours of water flow) according to the Algebraic yPlus, L-VEL, Spalart-Allmaras turbulence models and the laminar flow equation.

Conclusion

The following conclusions were made based on the performed analysis of the modeling results of flow of two different fluids in the pipeline with the local resistance:

1. Initial flow velocity of water and industrial oil of 1 m/s and the expansion angle of the diffuser of 18 degrees do not lead to the formation of intense vortex flows. Regime of water flow according to the calculated Reynolds number is closer to transition regime, while regime of industrial oil flow is laminar.
2. Flow of industrial oil retains its shape along the entire length of the considered section of the pipeline, but flow intensity decreases in the diffuser. Water flow retains its intensity and shape both in the diffuser and at the some distance after the expanding part.
3. The calculation features according to the Spalart-Allmaras turbulence model are presented by increasing flow velocity of industrial oil, and decreasing flow velocity of water under the same modeling conditions.

References:

1. Idel′chik, E. (1996). Handbook of Hydraulic Resistance. *Begell House*, p. 790.
2. (n.d.). State system for ensuring the uniformity of measurements. Measurement of liquids and gases flow rate and quantity by differential pressure method. *Orifice plates, nozzles ISA 1932 and Venturi tubes inserted in circular cross-section filled conduits. Specifications*.
3. Chemezov, D. A., & Bayakina, A. V. (2014). Simulation modeling of water flow in the Venturi nozzle. *ISJ Theoretical & Applied Science, 07 (15)*, 25-29.
4. Chemezov, D. (2016). The character of the fluid flow in the pipelines with the local hydraulic resistances. *ISJ Theoretical & Applied Science, 12 (44)*, 62-68.
5. Bardina, J. E., Huang, P. G., & Coakley, T. J. (1997). Turbulence Modeling Validation, Testing, and Development. *NASA Technical Memorandum, 110446*.
6. Bradshaw, P., Launder, B. E., & Lumley, J. L. (n.d.). Collaborative testing of turbulence models, *AIAA-91-0215*.
7. Towsend, A. A. (1976). The structure of turbulent shear flow. *Cambridge University Press, New York*.
8. Bredberg, J., Peng, S.-H., & Davidson, L. (2002). An improved k-ω turbulence model applied to recirculating flows. *International Journal of Heat and Fluid Flow, 23, 6*, 731-743.
9. Spalart, P. R., & Allmaras, S. R. (1994). A one-equation turbulence model for aerodynamic flows. *La Recherche Aérospatiale, №1*, 5-21.
10. Spalart, P. R. (2000). Strategies for turbulence modelling and simulations. *Int. J. Heat and Fluid Flow, vol. 21, iss. 3*, 252-263.